Using conformationally locked nucleosides to calibrate the anomeric effect: implications for glycosyl bond stability

Hyung Ryong Moon [a,†], Maqbool A. Siddiqui [a], Guangyu Sun [a,‡], Igor V. Filippov [b], Nicholas A. Landsman [a,§], Yi-Chien Lee [a,¶], Kristie M. Adams [a], Joseph J. Barchi, Jr. [a], Jeffrey R. Deschamps [c], Marc C. Nicklaus [a], James A. Kelley [a], Victor E. Marquez [a,*]

[a] Chemical Biology Laboratory, Center for Cancer Research, National Cancer Institute at Frederick, NIH, USA
[b] SAIC-Frederick, Inc., Frederick, Maryland MD 21702, USA
[c] Naval Research Laboratory, Washington DC 20375, USA

ARTICLE INFO

ABSTRACT

Steric and electronic parameters, such as the anomeric effect (AE) and *gauche* effect play significant roles in steering the North⇆South equilibrium of nucleosides in solution.
Two isomeric oxa-bicyclo[3.1.0]hexane nucleosides that are conformationally locked in either the North or the South conformation of the pseudorotational cycle were designed to study the consequences of having the AE operational or not, independent of other parameters. The rigidity of the system allowed the orientation of the orbitals involved to be set in 'fixed' relationships, either antiperiplanar where the AE is permanently 'on', or *gauche* where the AE is impaired. The consequences of these two alternatives were subjected to high-level calculations and measured experimentally by X-ray crystallography, hydrolytic stability of the glycosyl bond, and pK_a values.

Published by Elsevier Ltd.

1. Introduction

In β-D-nucleosides, the O4′–C1′–N1/N9 anomeric effect (AE) is characterized by the orbital interaction between the lone pair of the endocyclic O4′ and the highest p-orbital component of the antibonding orbital of the C1′–N1/N9 glycosyl bond ($n_{O4'} \rightarrow \sigma^*_{C1'-N1/N9}$).[1,2]Such orbital interaction is very much dependent on the conformation of the nucleoside. For example, in 2′,3′-dideoxyadenosine (ddA), the AE is the strongest when the conformation of the nucleoside is North (Fig. 1) and it would tend to drive the two-state North⇆South equilibrium of ddA towards a North conformation.[3,4] However, because the rapid North⇆South equilibrium is subject to other stereoelectronic interactions, it is difficult to assess the isolated role and consequences of the AE by itself in a given conformation.

Carbocyclic nucleosides constructed on a bicyclo[3.1.0]hexane template can lock the conformation of the embedded cyclopentane ring at either antipode (North and South) of the pseudorotational cycle,[5] but obviously in this instance there is no AE. Hence, the introduction of an oxygen at a suitable position on the scaffold was envisaged to restore the AE in the resulting oxo-bicyclo[3.1.0]hexane template and fix the position of the oxygen's lone pair into (1) an antiperiplanar orientation where the AE would be permanently 'on', or (2) a *gauche* orientation where the AE would be permanently 'off' (Fig. 2). The synthesis and study of these two target compounds in terms of the stability of the glycosyl bond, which is intrinsically associated with the presence or absence of the AE, is the subject of this work.[6]

2. Results and discussion

2.1. Synthesis

Both compounds (±)-**1** and (±)-**2** were conveniently synthesized in racemic form, as the relative spatial orientation of the orbitals would be identical for each set of enantiomers.

---

* Corresponding author. E-mail address: marquezv@mail.nih.gov (V.E. Marquez).
† Present address: Laboratory of Medicinal Chemistry, College of Pharmacy and Research Institute for Drug Development, Pusan National University, Busan 609-735, Republic of Korea.
‡ Present address: Vecna Technologies, Inc., 6404 Ivy Lane, Suite 500, Greenbelt, Maryland MD 20770, USA.
§ Present address: Keck School of Medicine, University of Southern California, 1975 Zonal Avenue, Los Angeles, California CA 90089, USA.
¶ Present address: Lombardi Cancer Comprehensive Center, Georgetown University Medical Center, 3970 Reservoir Rd. NW, Washington DC 20057, USA.
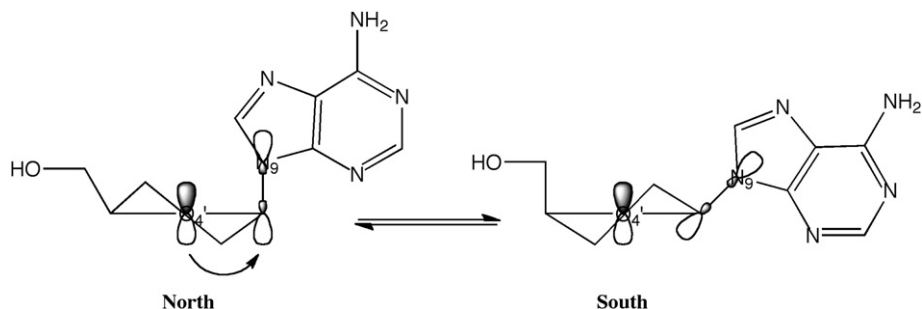
Figure 1. The anomeric effect (AE) between the antiperiplanar (p-type) O4′-lone pair and the C1′−N9 bond is most efficient (curved arrow) when ddA adopts the North conformation.
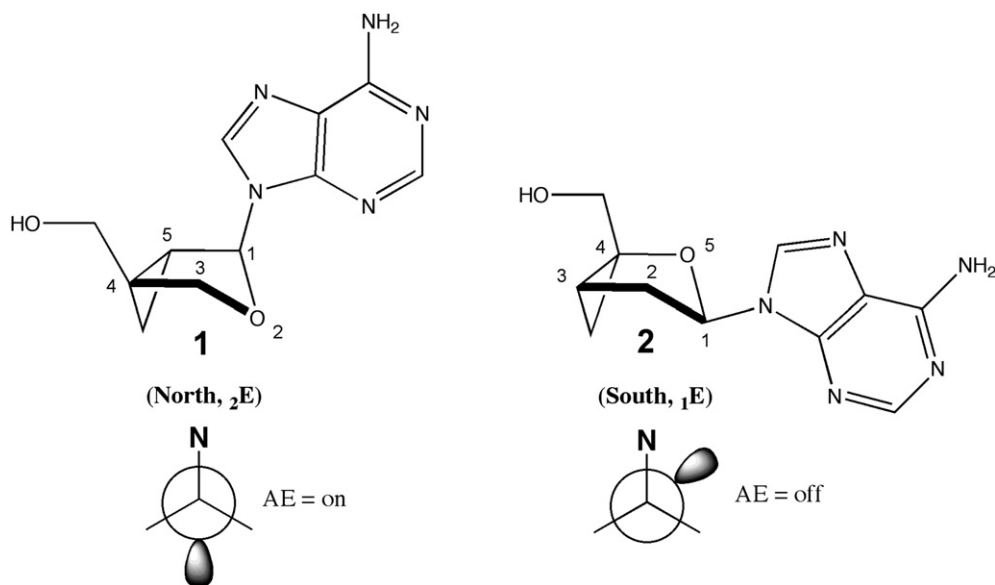

Figure 2. Oxo-bicyclo[3.1.0]hexane nucleosides where the AE is 'on' (North, compound **1**) and 'off' (South, compound **2**). The numbering and notation of the puckered tetrahydrofuran envelope embedded in the structure ($_2$E and $_1$E) is shown. The Newman projections show the antiperiplanar and gauche disposition of the lone pair relative to the C−N bond in **1** and **2**, respectively.

For the first target [(±)-**1**], the synthesis started with the bis-silyl protected, conjugated ester **3** (Scheme 1) that was synthesized according to the procedure of Jeong et al.[7]

Reduction to the allylic alcohol **4** and cyclopropanation under modified Simmons/Smith conditions[8] provided the {2,2-bis[(*tert*-butyldimethylsilyloxy)methyl]cyclopropyl}-methanol [(±)-**5**]. Swern oxidation[9] of the primary alcohol generated aldehyde (±)-**6**, which under mild acidic conditions cyclized almost quantitatively to the racemic lactol (±)-**7**. Treatment of (±)-**7** with acetic anhydride gave exclusively the diacetate (±)-**8** (Scheme 2). In both (±)-**7** and (±)-**8**, the appearance of the anomeric proton (H-2, IUPAC numbering) was a singlet, thus confirming the axial disposition of the OH and OAc groups. The diacetate was coupled with *N*-benzoyladenine under Vorbrüggen conditions[10] (Scheme 2) to give, after column chromatography, a mixture of α,β-(±)-**9** (60%) and a smaller amount (18%) of second fraction that was assumed to be an epimeric mixture of the minor N7 isomer. After removal of the acyl groups with methanolic ammonia, separation of (±)-**1** (60%) from the corresponding α-isomer (15%) was achieved after column chromatography. Consistent with the β-stereochemistry and the pseudoboat conformation of the oxo-bicyclo[3.1.0]hexane template, the anomeric proton (H-4, IUPAC numbering) in (±)-**1** was a singlet while the corresponding anomeric proton for the α-isomer resonated as a doublet (*J*=2.7 Hz).
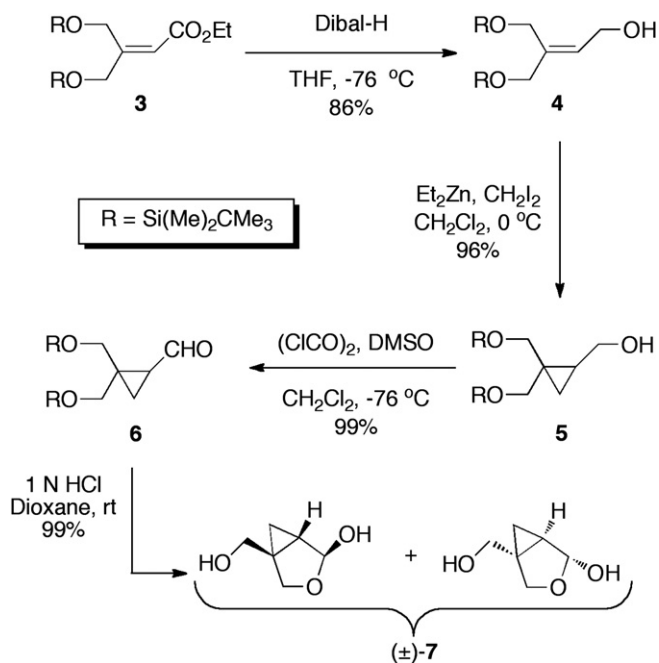

Scheme 1.
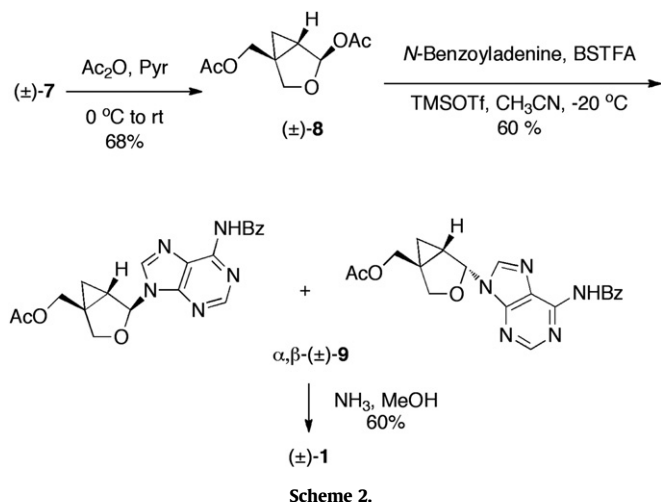
Scheme 2.

The synthesis of the second target [(±)-**2**] started with 1-methyl 5-*O*-benzoyl-D-ribofuranoside (**10**, mixture of anomers), which was prepared from 2-deoxy-D-ribose according to the literature[11] (Scheme 3). After exchanging protective groups to selectively free the 5′-OH,[12] a PhI(OAc)2/TEMPO oxidation[13] afforded the methyl ester **12** and set the stage for the elimination of the secondary alcohol to give the corresponding 4,5-dihydrofuran-2-carboxylate
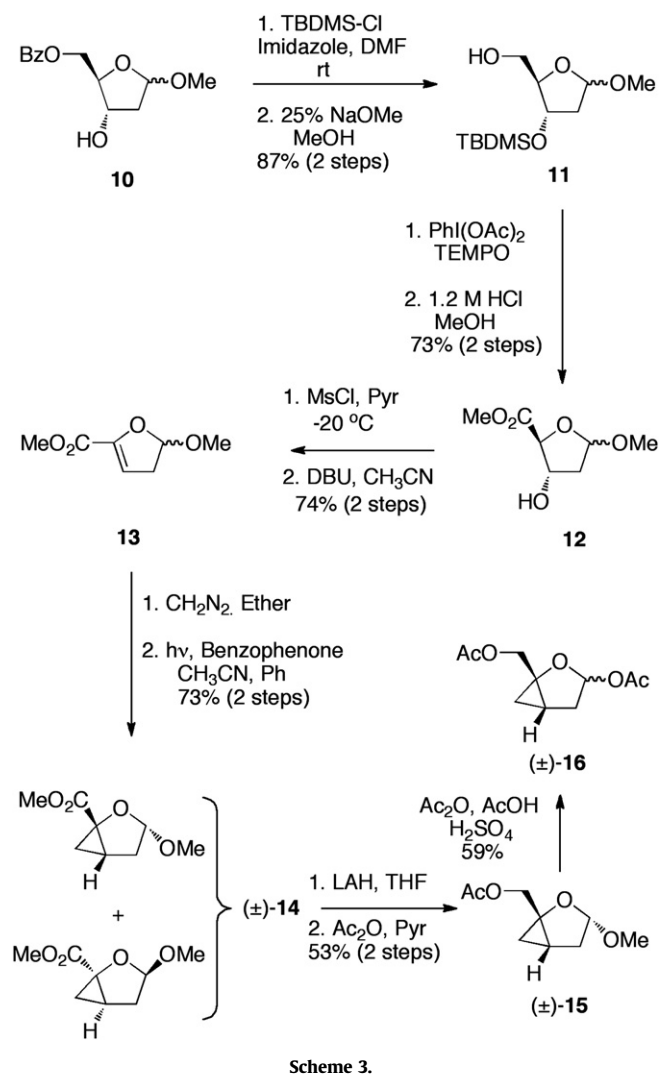
ester **13** in two steps. The 1,3-dipolar cycloaddition of diazomethane to **13** gave the *cis*-fused pyrazoline intermediate, which without isolation underwent photolysis-induced nitrogen extrusion to give exclusively the racemate (±)-**14**. Here again, because the axial orientation of the OMe reduces the second coupling constant to zero, the anomeric proton (H-3, IUPAC numbering) presented a doublet (J=6.3 Hz). Hydride reduction of the ester in (±)-**14**, followed by treatment with acetic anhydride, gave the pseudosugar precursor (±)-**15** (drawn in Scheme 3 as one enantiomer), which also displayed the anomeric proton as a doublet (J=5.9 Hz). Since acetyl glycosides are better coupling reagents with nucleobases, the anomeric OMe was converted to the acetate under acid-catalyzed conditions in the presence of acetic anhydride to give (±)-**16** as a 2:1 mixture of α,β-isomers (Scheme 3). The coupling of the α,β-mixture of (±)-**16** with adenine provided a mixture of only N_9-isomers that was separated by column chromatography after converting the mixture to the corresponding N^6-benzoyladenine derivatives prepared by the transient protection procedure of Jones et al.[14] (Scheme 4). The anomeric protons (H-3, IUPAC numbering) in both the major β-isomer [(±)-**2**] and the minor α-isomer appeared as similar doublet-of doublets with coupling constants of J=7.3, 4.9 Hz, and J=7.9, 5.4 Hz, respectively. This was consistent with the expected dominant pseudoboat conformation for the oxo-bicyclo[3.1.0]hexane template in both anomers. However, the close similarity of the coupling constants complicated the straightforward identification of the desired β-isomer [(±)-**2**].

Scheme 3.

Scheme 4.
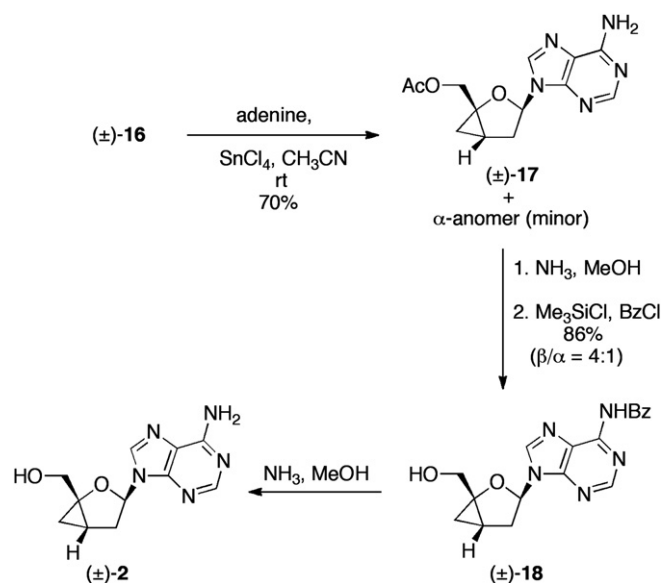
With the aid of 1-dimensional NOE experiments, it was possible to identify the desired target. The most diagnostic NOE was that between the anomeric proton and the *endo* proton located at the tip of the fused cyclopropane ring. This was observed only for the β-isomer (±)-**2** (Fig. 3).

2.2. X-ray crystallography

The crystal structure of (±)-**1** allowed us to confirm all the assignments made by ^{1}H NMR spectroscopy as well as the boat disposition of the oxo-bicyclo[3.1.0]hexane template (Fig. 4). Similarly, it allowed us to measure the corresponding bond lengths that would be affected by the presence of a conformationally fixed AE. Indeed in (±)-**1**, the AE is permanently 'on', which was reflected by
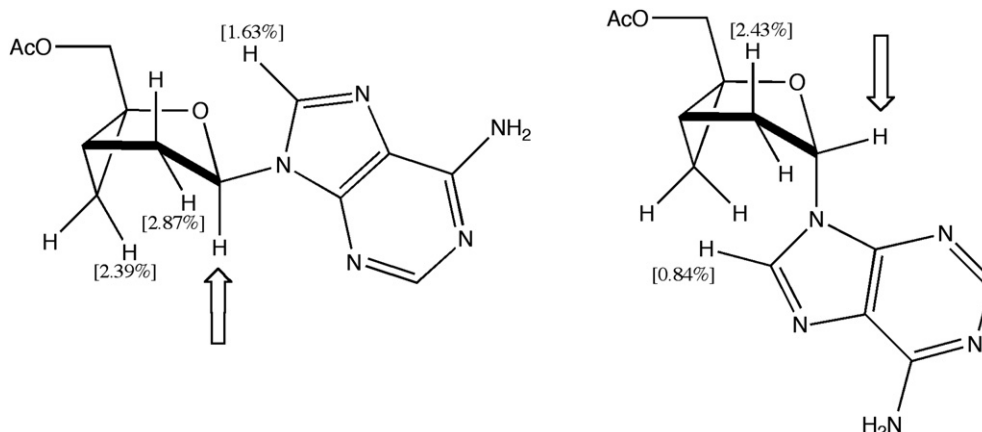
Figure 3. Important NOE enhancements (%) resulting from the irradiation of the anomeric proton (arrow) in (±)-**2** (left) and the α-isomer (right).

the corresponding shortening of the C4′-O3′ bond (1.413 Å) compared to the uninvolved C2′-O3′ bond (1.451 Å). Also, as a consequence of the AE, the length of the C4′−N9 bond increased slightly (1.475 Å) relative to, for example, the C−N bond length of the corresponding bicyclo[3.1.0]hexane nucleoside (1.470 Å).[15]

Figure 4. View of (±)-**1** (one enantiomer) based on the results of the X-ray study. Displacement ellipsoid plot drawn at the 50 % level and the numbering system corresponds to the IUPAC name (see Experimental).

A direct comparison of bond lengths between (±)-**1** and (±)-**2** could only be made from calculated structures as discussed in the following section because we were unable to obtain good quality crystals for (±)-**2**. However, the reliability of the computed values (vide infra) was excellent as corroborated by comparing the C4′−N9

bond distance in the crystal structure of (±)-**1** (1.475 Å) with the calculated value of 1.482 Å (Δ=0.007 Å).

2.3. Calculated interactions between the n_{sp2} oxygen lone pair and the glycosyl bond

The interaction between the oxygen's lone pair and the adjacent bonds was studied computationally. The lone pair natural bond orbitals (NBOs)[16] for the ring oxygen in (±)-**1** and (±)-**2** are shown in Figure 5. Two lone pairs exist for each oxygen atom: one lower-energy lone pair (n1) with more s character than the other lone pair (n2), which is almost entirely p character.

A strong AE ($n_O \rightarrow \sigma^*_{C-N}$) would allow the oxygen to participate in hyperconjugation with the sp^2 hybridized (n2) lone pair. This interaction will be strongest if this p-type orbital is in a fixed antiperiplanar orientation relative to the C−N bond as seen for (±)-**1** in Figure 5. Indeed, the calculations shown in Table 1 indicate that (±)-**1** has a strong lone pair−empty antibonding orbital interaction ($n2 \rightarrow \sigma^*_{C-N}$) of 13.5 kcal/mol. This interaction is also reflected in the lengthening of the C−N bond (1.482 Å), which is agreement with the X-ray structure. Protonation strengthens this interaction (16.9 kcal/mol) and the C−N bond (1.516 Å) has a longer equilibrium value than in the neutral nucleoside. Conversely, the lone pair−empty antibonding orbital interaction ($n2 \rightarrow \sigma^*_{C-N}$) for (±)-**2** amounts to only 4.2 kcal/mol due to the *gauche* alignment of the orbitals. As a consequence of the lack of AE, the length of the C−N bond appears shorter (1.448 Å); as before, protonation of (±)-**2** increases the orbital interaction but to a lesser extent.

It is important to recognize that hyperconjugation is not limited to a single lone pair although within the threshold limits that NBO analysis uses, the magnitude depends on the absolute value of the cosine of the angle between the overlapping orbitals. This interaction is more effective in the antiperiplanar relationship.

For comparison, the same calculations were performed for ddA by restricting its conformation to the North or the South hemisphere. As shown in Table 1, the strongest. AE interaction occurs only when ddA adopts the North conformation. However, because of the rapid North⇋South equilibrium in ddA the magnitude of the net AE in this case is difficult to estimate.

2.4. Depurination kinetics

A direct consequence of the strong AE in the North conformations, which is in keeping with the lengthening of the C−N bond, is the expected ease of cleavage of the glycosyl bond under acidic
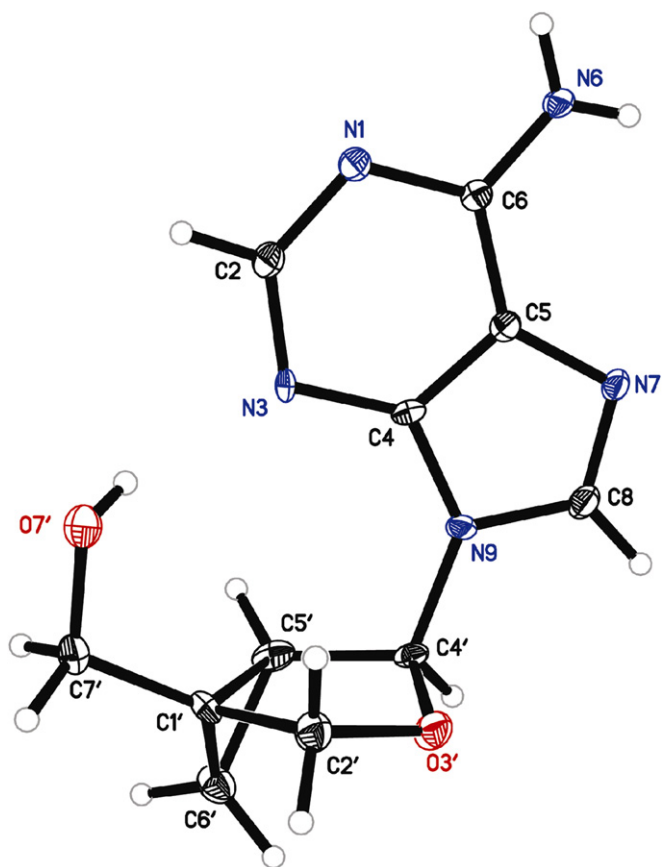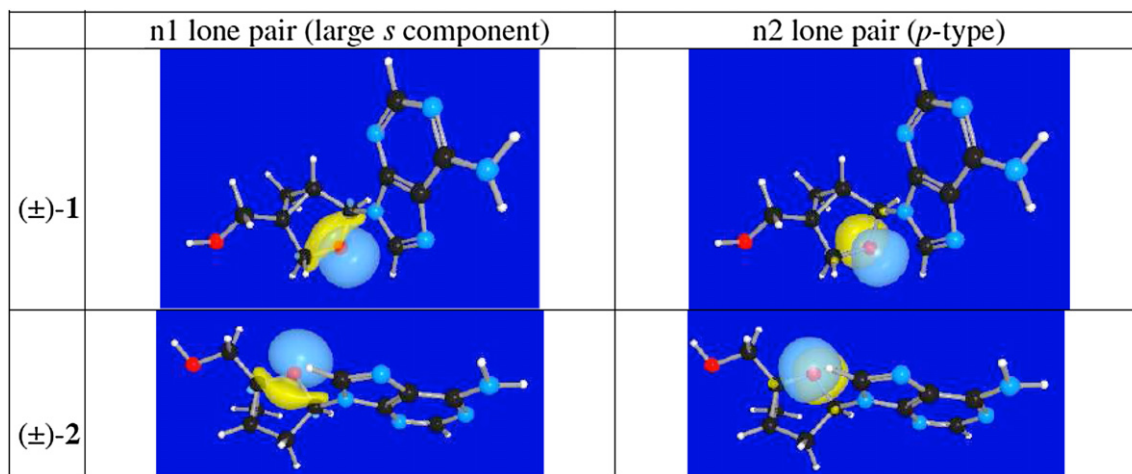
Figure 5. NBO lone pair orbitals of (±)-**1** and (±)-**2**.

Table 1
Leading second order perturbation interactions between the oxygen lone pair and the antibonding orbital of the glycosyl (C–N) bond for neutral and protonated molecules. The calculated pseudorotational parameters (P and ν_{max})[17] and the Hartree-Fock (HF) ground state energies are also shown

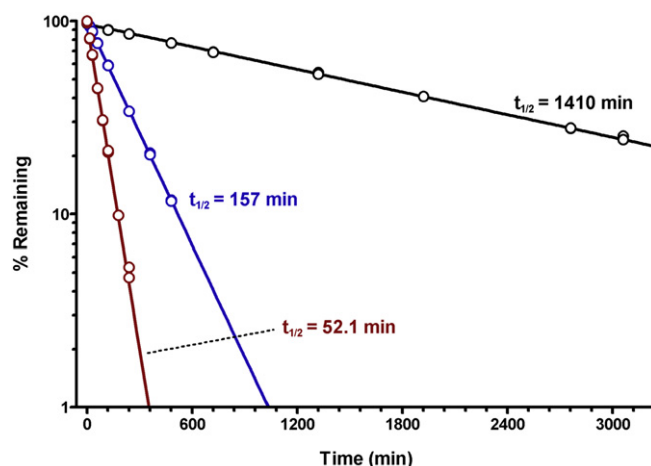|	
(±)-**1** (locked-North)	(±)-**1** (locked-North)+H^+
$P=340.17°$ ($_2$E), $\nu_{max}=30.11°$	$P=342.30°$ ($_2$E), $\nu_{max}=25.06°$
HF=−851.1701093	HF=−851.5533015
n2 → $\sigma*_{C-N}$=13.5 kcal/mol	n2 → $\sigma*_{C-N}$=16.9 kcal/mol
C–N bond=1.4820 Å	C–N bond=1.5162 Å
(±)-**2** (locked-South)	(±)-**2** (locked-South)+H^+
$P=129.22°$, ($_1$E), $\nu_{max}=23.14°$	$P=129.78°$, ($_1$E), $\nu_{max}=21.70°$
HF=−851.1661996	HF=−851.5498595
n2→$\sigma*_{C-N}$=4.2 kcal/mol	n2→$\sigma*_{C-N}$=6.0 kcal/mol
C–N bond=1.4486 Å	C–N bond=1.4782 Å
ddA (North)	ddA (North)+H^+
$P=358.29°$ (^{3}T$_2$), $\nu_{max}=35.76°$	$P=11.26°$ (^{3}T$_2$), $\nu_{max}=35.40°$
HF=−813.0985834	HF=−813.4829554
n2→$\sigma*_{C-N}$=12.2 kcal/mol	n2→$\sigma*_{C-N}$=13.7 kcal/mol
C–N bond=1.4803 Å	C–N bond=1.5079 Å
ddA (South)	ddA (South)+H^+
$P=160.24°$ (^{2}E), $\nu_{max}=35.73°$	$P=172.35°$ (^{2}T$_3$), $\nu_{max}=34.74°$
HF=−813.0972147	HF=−813.4814849
n2→$\sigma*_{C-N}$=4.4 kcal/mol	n2→$\sigma*_{C-N}$=7.8 kcal/mol
C–N bond=1.4521 Å	C–N bond=1.4877 Å

Figure 6. Normalized stability comparison of the depurination kinetics of (±)-**1** (blue line), (±)-**2** (black line) and ddA (red line) at pH 3, 37 °C determined by HPLC.

conditions. Thus, compound (±)-**1** was expected to hydrolyze faster than its counterpart (±)-**2**. Indeed, (±)-**2** for which the AE is significantly reduced was quite stable showing a half-life of 1,410 min at pH 3 (Fig. 6), while (±)-**1** with a strong AE was cleaved with a half-life of 157 min at the same pH. At pH 2 the half-lives were 52.8 min and 6.46 min, respectively (not shown). The lower half-life for ddA (52.1 min at pH 3) presents an interesting quandary since one would have expected compound (±)-**1** with the locked AE to depurinate faster than ddA. Furthermore, the cyclopropylcarbinyl cation stabilization ought to make the cation in (±)-**1** even more stable than that in ddA!

However, one has to consider the additional issue of ring strain associated with changing an sp^3 center to an sp^2 center within a bicyclic system compared to the monocycle. Therefore, we propose that the increased ring strain in (±)-**1** outweighs cation stabilization.

In order to corroborate our hypothesis, the following isodesmic reactions were studied (Fig. 7). In the first set of reactions (A⇆B) the exothermic change in an open chain system shows that the cyclopropylcarbinyl cation is indeed more stable. However, when the same system is embedded in a strained bicyclic system, as in the second reaction (C⇆D), the oxocarbenium is less stable than in a strain-free monocyclic system. These results are in agreement with the proposed increase in ring strain in (±)-**1**, which diminishes cation stabilization relative to ddA.

2.5. pK_a values

It has been shown by Chattopadhyaya et al. that alterations in the electronic properties of the nucleobase in conventional nucleosides, from neutral to protonated, are effectively transmitted to the pentofuranose moiety through the AE and manifested in changes in the N⇆S equilibrium.[18,19] Because the AE is more effectively transmitted when the conformation of the sugar is North, the thermodynamics of the N⇆S equilibrium as a function of pH (pD in most NMR experiments) provides a direct measurement of the pK_a of the nucleobase. The pK_a values experimentally calculated from changes in $\Delta G°$ of the N⇆S equilibrium for 2′-deoxyadenosine and adenosine were the same (pK_a=3.5), which compared well with the pK_a value calculated from changes in the chemical shift of the H8 and H2 protons as a function of pD (pK_a=3.6).[19] Because in compounds (±)-**1** and (±)-**2** the AE would be locked 'on' and 'off', respectively, we anticipated that perhaps
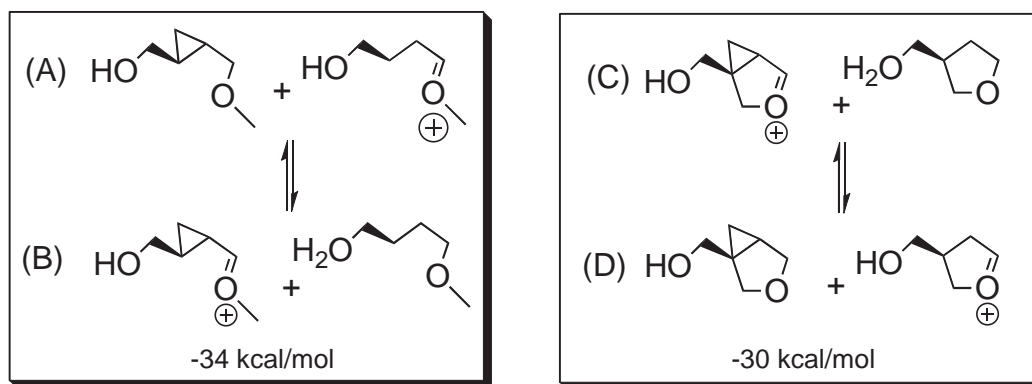
Figure 7. Proposed isodesmic reactions to explore ring strain changes associated with changing an sp[3] center to an sp[2] center in the bicyclic system compared to the monocyclic system. Both reactions are exothermic in the A→B and C→D directions.

there would be measurable differences in the pK_a values of (±)-**1** and (±)-**2** determined by following the changes in chemical shift of the H8 and H2 protons (Supplementary Fig. 1). The pK_a values, however, were only 0.14 log units apart, which suggest that the cationic charge is so stabilized by the purine system that the small perturbation due to hyperconjugation contributes much less to modify the charge distribution of the nucleobase.

3. Conclusions

By exploiting the rigid nature of the oxo-bicyclo[3.1.0]hexane template we have constructed two nucleosides [(±)-**1** and (±)-**2**] where for the first time the consequences of having an operational or nonfunctional AE, independent of steric or other electronic parameters, have been studied. The penalty of having an operational AE had a direct impact on the hydrolytic stability of the C–N bond, which was less stable when the anomeric effect was permanently 'on'. This was achieved only in the North conformation of (±)-**1**. Conversely, the stability of the nucleoside where the anomeric effect was 'off', as in the South conformation of (±)-**2**, was enhanced. This result provides a strategy to increase the hydrolytic stability of nucleosides by simply steering the orbitals involved in the AE into a *gauche* relationship. In the case of the oxo-bicyclo[3.1.0]hexane nucleosides discussed here these changes are permanently fixed. However, in conventional nucleosides appropriate substitutions on the ribose ring with various groups that control steric and electronic parameters could steer the conformation of the nucleoside to the South where hydrolytic stability will be significantly improved.

4. Experimental section

4.1. X-ray Crystal structure of (±)-1

Single-crystal X-ray diffraction data were collected at 93 °K using Mo Kα radiation and a Bruker SMART 1000 CCD area detector. A 0.24×0.10×0.05 mm^3 crystal was prepared for data collection coating with high viscosity microscope oil (Paratone-N, Hampton Research). The oil-coated crystal was mounted on a glass rod and transferred immediately to the cold stream (−180 °C) on the diffractometer. The crystal was monoclinic in space group $P2_1/c$ with unit cell dimensions a=13.3584 (14) Å, b=7.6729 (8) Å, c=10.9025 (11) Å, and β=101.570(2)°. Corrections were applied for Lorentz, polarization, and absorption effects. Data were 97.2% completed to 28.29°θ (approximately 0.75 Å) with an average redundancy of 2.98. The structure was solved by direct methods and refined by full-matrix least squares on F^2 values using the programs found in the SHELXTL suite (Bruker, SHELXTL v6.10, 2000, Bruker AXS Inc.,

Madison, WI). Parameters refined included atomic coordinates and anisotropic thermal parameters for all non-hydrogen atoms. Hydrogen atoms on carbons were included using a riding model [coordinate shifts of C applied to H atoms] with C–H distance set at 0.96 Å. The asymmetric contains a single molecule of **1**. Atomic coordinates for compound **1** have been deposited with the Cambridge Crystallographic Data Centre (deposition number 739340). Copies of the data can be obtained, free of charge, on application to CCDC, 12 Union Road, Cambridge CB2 1EZ, UK [fax: +44 1223 336033 or e-mail: deposit@ccdc.cam.ac.uk.

4.2. NOE measurements

GOESY (DPFGSE-NOE)[20] experiments were carried out on a Varian Unity INOVA 400 NMR spectrometer, with an operating frequency of 399.74 MHz. Samples were dissolved in D$_2$O, and were not degassed prior to data accumulation. Experiments were performed at 25 °C with 500 ms mixing time, and 1024 or 13000 scans were recorded, depending on sample concentration. Spectra were internally referenced to 2,2-dimethyl-2-silapentane-5-sulfonic acid (DSS) at 0.0 ppm.

4.3. pK_a Determinations

^{1}H NMR experiments for the pK_a determinations were recorded on a Varian Inova 500 instrument in D$_2$O solution at 1.5 mmol nucleoside concentrations. The pH titration studies were performed over the range of pH 1.6–8.0 with 0.3–0.5 pH interval. The pH of the samples was adjusted with small volumes of either DCl or NaOD solutions in D$_2$O. All 1D spectra were collected with 64 K data points with dioxane-d_8 (δ=3.750 ppm) as an internal reference. The plot of pH versus ^{1}H chemical shifts shows a sigmoidal behavior and the pK_a values were determined by Hill plot analysis as previously described.[19] The pK_a values were calculated based on the equation:

$$\mathrm{pH} = \log[(\Delta HX_{Tot} - \Delta_{HX}/\Delta_{HX})] + \mathrm{p}K_a$$

where ΔHX_{Tot} is the chemical shift difference between the neutral and fully protonated state of proton X. These calculations were performed using Origin 7 (Northampton, MA).

4.4. Interactions between the n$_{sp2}$ oxygen lone pair and the glycosyl bond

The interaction between the oxygen lone pairs of the sugar oxygen and adjacent bonds were studied using Gaussian 98[21] and NBO5.0.[16]The geometries of the molecules (Table 1) were optimized

at the B3LYP/6-31G* level of theory and the natural bond orbitals were plotted using NBOView program.

4.5. Isodesmic reactions

The geometry optimization and zero-point energy calculations were performed using Gaussian 03[22] at the B3LYP/6-31G* level of theory.

4.6. Depurination kinetics

Glycosyl bond stability was determined for 2′,3′-dideoxy-adenosine (ddA) and for compounds **1** and **2** at both pH 2 and 3 by following the hydrolysis of the parent nucleoside and the concomitant formation of adenine using reversed-phase HPLC with UV detection. (Details of the HPLC analysis are available in the Supplementary data). Microscale hydrolysis reactions were carried out for each compound individually in 1.5 mL screw-cap Eppendorff tubes that were pre-equilibrated with buffer at 37 °C before being charged with substrate (60 μg/mL, 0.24–0.25 mM) and guanosine internal standard (25 μg/mL, 0.088 mM). Reaction mixture pH was maintained with either a 100 mM pH 2 HCl/glycine buffer or with a 100 mM pH 3 potassium citrate buffer. Appropriate kinetic sampling times were based on prior survey reactions and varied for each compound and each pH. Seven to nine 160 μL reaction mixture aliquots were taken at predetermined times to define a kinetic profile, with the first being obtained immediately after addition of substrate (t=0). Following acquisition of the initial sample, the Eppendorf reaction tube was tightly sealed and placed into an equilibrated tube heater. Prior to each subsequent sampling, the reaction tube was gently vortexed to insure complete mixing and then quickly centrifuged to collect any condensate from the sides and top. Each sample aliquot was placed in a 1.5 mL Eppendorf tube and then immediately quenched with twice the volume (e.g., 320 μL) of 500 mM pH 7.0 KH$_2$PO$_4$, vortexed to mix, and then frozen on dry ice until analysis. Following HPLC analysis of the timed reaction samples, both substrate (nucleoside) disappearance and product (adenine) appearance profiles were constructed using the ratio of analyte peak area to that of the guanosine internal standard. These profiles were curve-fit to a first-order exponential decay or appearance function as appropriate using GraphPad Prism software (Version 4.03). All duplicate points were considered individually and non-linear least-squares curve fitting typically gave correlation coefficients of $r^2 >$0.998 for all cases. The appropriate rate constants and half-lives were then calculated from these curves.

4.7. General chemistry

All reagents and solvents purchased were of the highest commercial quality and used without further purification unless otherwise stated. Column chromatography was performed on silica gel 60, 230–400 mesh (E. Merck). ^{1}H and ^{13}C NMR spectra were either on a Bruker AC250 at 250 MHz or a Varian Inova instrument at 400 MHz. ^{13}C NMR spectra were recorded on the Varian Inova 400 at 100 MHz. Spectra were referenced to the solvent in which they were run (7.24 ppm for CDCl$_3$). Spectral assignments were obtained from 2-dimensional homonuclear correlation data. Positive ion fast-atom bombardment mass spectra (FAB MS) were obtained on a VG 70-SE double-focusing mass spectrometer operated at an accelerating voltage of 8 kV under the control of a MASPEC-II[32] data system for Windows (MasCom GmbH, Bremen, Germany). Either glycerol or 3-nitrobenzyl alcohol was used as the sample matrix, and ionization was effected by a 2-μA beam of cesium ions generated in a focused ion gun at operated at 27±2 kV. The FAB mass spectra of all analyzed compounds indicated either

a molecular species [M+H]$^+$ or fragment ions highly indicative of structure. Nominal mass MS were obtained at a resolution of 1500, and matrix-derived ions were background subtracted during data system processing. Positive-ion atmospheric pressure chemical ionization (APCI) and electrospray ionization (ESI) mass spectra were obtained on an Agilent LC/MSD single quadrupole system equipped with a multi-mode ion source. Samples were run as solutions by flow-injection-analysis (FIA) into a 300 μL/min flow of 50% CH$_3$OH/H$_2$O containing 0.1% (v/v) acetic acid, which was then ionized by either APCI or ESI. APCI employed a corona needle current of 4.0 μA, a charging voltage of 2 kV, and a nozzle-skimmer potential (fragmentor voltage) of 70 V; while ESI used a capillary voltage of 4 kV and a fragmentor voltage of 100 V. The high-purity nitrogen nebulizer pressure, drying gas flow rate and drying gas temperature were set appropriately for the ionization method. Elemental analyses were performed by Atlantic Microlab, Inc., Atlanta, GA.

4.7.1. 4-(tert-Butyldimethylsilyloxy)-3-[(tert-butyldimethylsilyloxy)methyl]but-2-en-1-ol (4). A stirred solution of ester **3**[7] (11.36 g, 30.3 mmol) in THF (240 mL) was treated with DIBAL-H (66.7 mL, 1 M solution in THF) at −78 °C. After 1 h, methanol (60 mL) and EtOAc (600 mL) were added and the solution was further stirred at room temperature overnight. The obtained gel was filtered through a pad of Celite® and the collected filtrate was concentrated under reduced pressure. The residue was purified by silica gel flash column chromatography (hexanes/EtOAc, 10:1) to give **4** (9.0 g, 86%) as a clear oil; δ_H (250 MHz, CDCl$_3$) 5.91 (irregular t, J=6.7 Hz, 1H, C=CH), 4.31 (irregular t, J=3 Hz, 4H, 2×SiOCH_2), 4.24 (s, 2H, CH_2OH), 1.00 (s, 9H, C(CH_3)$_3$), 0.98 (s, 9H, C(CH_3)$_3$), 0.17 (s, 6H, 2×CH_3), 0.16 (s, 6H, 2×CH_3); δ_C (100 MHz, CDCl$_3$) 141.3, 125.7, 65.0, 59.6, 58.8, 26.1, 26.0, 18.6, 18.4, −5.1, −5.2; FAB-MS m/z 347 (MH$^+$, 12%), 73 (100). Elemental analysis for C$_{17}$H$_{38}$O$_3$Si$_2$·0.1H$_2$O: calculated: C, 58.06; H, 10.95. Found: C, 58.18; H, 10.92.

4.7.2. {2,2-Bis[(tert-butyldimethylsilyloxy)methyl]cyclopropyl}methanol (5). Diiodomethane (10.5 mL, 130 mmol) was added dropwise to a solution of Et$_2$Zn (65 mL, 1 M solution in hexane) in CH$_2$Cl$_2$ (210 mL) at 0 °C while stirring. After 10 min, allylic alcohol **4** (9.0 g, 26 mmol) was added dropwise and stirring continued for 30 min at the same temperature. While still at 0 °C, the reaction was quenched with a saturated solution of NH$_4$Cl (30 mL) and the resulting mixture was partitioned between EtOAc (400 mL) and water (100 mL). The organic layer was dried (MgSO$_4$), filtered, and evaporated. The resulting residue was purified by silica gel column chromatography (hexanes/EtOAc, 6.5:1) to give **5** (9.03 g, 96%) as a clear oil; δ_H (250 MHz, CDCl$_3$) 4.36 (d, J=11.0 Hz, 1H, OCHHSi$_A$), 4.20 (dd, J=10.3, 1.5 Hz, 1H, CHHOH), 4.04 (td, J=11.5, 5.3 Hz, 1H, OCHHSi$_B$), 3.44 (dd, J=11.5, 1.3 Hz, 1H, OCHHSi$_B$), 3.29−3.39 (m, 2H, OCHHSi$_A$, OH), 2.93 (d, J=10.3 Hz, 1H, CHHOH), 1.27 (m, 1H, cyclopropane-CH), 1.00 (s, 9H, C(CH_3)$_3$), 0.97 (s, 9H, C(CH_3)$_3$), 0.78 (dd, J=8.5, 5.0 Hz, 1H, cyclopropane-CHH), 0.43 (td, J=5.1, 1.5 Hz, 1H, cyclopropane-CHH), 0.19 (s, 3H, CH_3), 0.17 (s, 3H, CH_3), 0.12 (s, 3H, CH_3), 0.11 (s, 3H, CH_3); δ_C (100 MHz, CDCl$_3$) 66.6, 63.5, 63.4, 29.0, 26.1, 26.0, 22.7, 18.5, 18.4, 14.5, −5.1, −5.2, −5.3, −5.4; FAB-MS m/z 361 (MH$^+$, 8%), 73 (100). Elemental analysis for C$_{18}$H$_{40}$O$_3$Si$_2$: calculated: C, 59.94; H, 11.18. Found: C, 59.94; H, 11.30.

4.7.3. 2,2-Bis[(tert-butyldimethylsilyloxy)methyl]cyclopropanecarbaldehyde (6). A commercial solution of oxalyl chloride (18.77 mL, 2 M solution in CH$_2$Cl$_2$) was diluted with additional CH$_2$Cl$_2$ (130 mL) and treated with DMSO (5.86 mL, 82.6 mmol) at −78 °C. After 20 min stirring at the same temperature, a solution of **5** (9.03 g, 25 mmol) in CH$_2$Cl$_2$ (50 mL) was added while the temperature was still maintained at −78 °C. Stirring was continued for 1 h, and, after the addition of triethylamine (21 mL, 150 mmol), the

temperature was gradually allowed to reach ambient conditions. The solution was then partitioned between ethyl ether (250 mL) and water (100 mL), and the organic layer was washed with brine (30 mL), dried (MgSO$_4$), filtered, and reduced to dryness. The residue was purified by silica gel column chromatography (hexanes/EtOAc, 20:1) to give aldehyde **6** (9.0 g, 99%) as a clear oil; δ_H (250 MHz, CDCl$_3$) 9.54 (d, J=4.9 Hz, 1H, CHO), 4.04 (d, J=10.9 Hz, 1H, OCHHSi$_A$), 3.89 (d, J=10.1 Hz, 1H, OCHHSi$_B$), 3.65 (d, J=10.9 Hz, 1H, OCHHSi$_A$), 3.53 (d, J=10.2 Hz, 1H, OCHHSi$_B$), 1.99 (dt, J=7.8, 5.1 Hz, 1H, cyclopropane-CH), 1.50 (t, J=5.0 Hz, cyclopropane-CHH), 1.28 (dd, J=7.8, 4.6 Hz, 1H, cyclopropane-CHH), 0.96 (s, 9H, C(CH$_3$)$_3$), 0.94 (s, 9H, C(CH$_3$)$_3$), 0.12 (s, 6H, 2×CH$_3$), 0.11 (s, 3H, CH$_3$), 0.09 (s, 3H, CH$_3$); δ_C (100 MHz, CDCl$_3$) 200.6, 64.5, 61.3, 37.7, 31.1, 26.0, 26.0, 18.4, 18.4, 16.3, −5.3, −5.3, −5.3, −5.4; FAB-MS m/z 301 (MH$^+$ −C$_4$H$_{10}$, 6%), 73 (100). Elemental analysis for C$_{18}$H$_{38}$O$_3$Si: calculated: C, 60.28; H, 10.68. Found: C, 60.27; H, 10.71.

4.7.4. (rel-1S,2S,5S)-5-(Hydroxymethyl)-3-oxabicyclo[3.1.0]hexan-2-ol [(±)-7].
A solution of aldehyde **6** (9.01 g, 25.1 mmol) in a mixture of 1,4-dioxane (42 mL) and 1 N HCl (42 mL) was stirred at room temperature for 16 h. The reaction mixture was neutralized with Dowex® anion exchange resin (OH$^-$) and filtered through a pad of Celite®. The filtrate was concentrated and the residue (3.26 g, 100%) was used in the following step without further purification. An analytical sample was obtained after silica gel flash column chromatography (CH$_2$Cl$_2$/MeOH, 22:1) to give pure (±)-**7** as a clear oil; δ_H (250 MHz, MeOH-d_4) 5.09 (s, 1H, H-2), 3.96 (d, J=8.1 Hz, 1H, H-4a), 3.81 (d, J=11.7 Hz, 1H, CHHOH), 3.74 (d, J=8.1 Hz, 1H, H-4b), 3.60 (d, J=11.7 Hz, 1H, CHHOH), 1.45 (dd, J=8.1, 3.9 Hz, 1H, H-1), 0.74 (ddd, J=8.1, 4.7, 0.7 Hz, 1H, H-6a), 0.43 (t, J=4.4 Hz, 1H, H-6b); δ_C (100 MHz, CD$_3$OD) 98.6, 68.8, 62.9, 29.8, 27.0, 11.8; FAB-MS m/z 113 (MH$^+$−H$_2$O, 100%) 83 (10). Elemental analysis for C$_6$H$_{10}$O$_3$·0.3H$_2$O: calculated: C, 53.17; H, 7.88. Found: C, 52.97; H, 7.81.

4.7.5. ((rel-1S,2R,5R)-5-(Acetyloxymethyl)-3-oxabicyclo[3.1.0]hexan-2-yl) acetate [(±)-8].
A stirred solution of lactol (±)-**7** (3.26 g, 25 mmol) in pyridine (25 mL) was treated with acetic anhydride (11.85 mL, 125.6 mmol) at 0 °C and allowed to reach room temperature. After 5 h, the volatiles were removed under reduced pressure and the residue was partitioned between EtOAc (200 mL) and water (50 mL). The organic layer was dried (MgSO$_4$), filtered, and evaporated. The crude material was purified by silica gel flash column chromatography (hexanes/EtOAc, 3:1) to give the diacetate (±)-**8** (3.64 g, 68%) as a clear oil; δ_H (250 MHz, CDCl$_3$) 6.16 (s, 1H, H-2), 4.48 (d, J=12 Hz, 1H, CHHOAc), 4.23 (d, J=12 Hz, 1H, CHHOAc), 4.10 (d, J=8.1 Hz, 1H, H-4a), 3.99 (d, J=8.3 Hz, 1H, H-4b), 2.17 (s, 3H, C(O)CH$_3$), 2.15 (s, 3H, C(O)CH$_3$), 1.77 (dd, J=8.5, 4.2 Hz, 1H, H-1), 0.97 (ddd, J=8.6, 5.3, 0.7 Hz, 1H, H-6a), 0.76 (t, J=4.9 Hz, 1H, H-6b); δ_C (100 MHz, CDCl$_3$) 171.1, 170.4, 98.9, 71.3, 65.2, 27.0, 26.6, 21.5, 21.0, 12.7; FAB-MS m/z 155 (MH$^+$−AcOH, 100%). Elemental analysis for C$_{10}$H$_{14}$O$_5$: calculated: C, 56.07; H, 6.59. Found: C, 56.43; H, 6.68.

4.7.6. α,β−[(rel-1R,5S)-3-Oxa-4-[6-(phenylcarbonylamino)purin-9-yl]bicyclo[3.1.0]hexyl}methyl acetate [α,β-(±)-9].
A suspension of N-benzoyladenine (348 mg, 1.45 mmol) in acetonitrile (5 mL) was treated with bis(trimethylsilyl)-trifluoroacetamide (BSTFA, 1 mL) and stirred at room temperature for 1 h until a clear solution was obtained. After removing the volatiles under reduced pressure and under anhydrous conditions, a solution of diacetate (±)-**8** (208 mg, 0.97 mmol) in acetonitrile (5 mL) was added and the resulting mixture was cooled to −20 °C before proceeding with the slow addition of trimethylsilyl trifluoromethanesulfonate (TMSOTf, 0.26 mL, 1.42 mmol). The stirred mixture was gradually allowed to reach room temperature and after 2 h, a saturated aqueous solution of NaHCO$_3$ was added. The mixture was filtered and the filtrate was extracted with CH$_2$Cl$_2$ and dried (MgSO$_4$). The organic solution was

reduced to dryness and the residue was purified by silica gel flash column chromatography (hexanes/EtOAc, 1:2) to give a mixture of α,β−(±)−**9** (230 mg, 60%) as a sticky oil and a smaller amount (67 mg, 18%) of second fraction that was deemed to be an epimeric mixture of the minor N$_7$-isomers.

4.7.7. [rel-(1S,4S,5S)-4-(6-Aminopurin-9-yl)-3-oxabicyclo[3.1.0]hexyl]methan-1-ol [(±)-1].
A solution of α,β−(±)−**9** (220 mg, 0.56 mmol) in saturated methanolic ammonia (6 mL) was stirred at room temperature overnight. The volatiles were removed and the residue was purified by silica gel flash column chromatography (CH$_2$Cl$_2$/MeOH, 9:1) to give (±)-**1** (83 mg, 60%) and the corresponding ∠-anomer (21 mg, 15%).

α-isomer [(±)-**1**]: white solid, mp 232−234 °C; δ_H (250 MHz, DMSO-d_6) 8.51 (s, 1H, H-8), 8.19 (s, 1H, H-2), 7.34 (br s, 2H, NH$_2$), 6.15 (s, 1H, H-4′), 5.29 (t, J=5.1 Hz, 1H, OH), 4.05 (d, J=8.3 Hz, 1H, H-2′a), 3.98 (dd, J=11.7, 5.0 Hz, 1H, CHHOH), 3.87 (d, J=8.3 Hz, 1H, H-2′b), 3.64 (dd, J=11.8, 5.1 Hz, 1H, CHHOH), 2.02 (dd, J=8.3, 4.1 Hz, 1H, H-5′), 1.00 (dd, J=8.2, 4.7 Hz, 1H, H-6′a), 0.70 (t, J=4.4 Hz, 1H, H-6′b); δ_C (62.5 MHz, DMSO-d_6) 155.9, 152.5, 149.0, 138.6, 118.7, 83.34, 69.03, 60.65, 31.27, 24.47, 12.59; FAB-MS m/z 248 (MH$^+$, 100%), 136 (b+2H$^+$, 36), 113 (26). Elemental analysis for C$_{11}$H$_{13}$N$_5$O$_2$: calculated: C, 53.43; H, 5.30; N, 28.32. Found: C, 53.60; H, 5.40; N, 28.05.

α-isomer white solid, mp 191−192 °C; δ_H (250 MHz, DMSO-d_6) 8.31 (s, 1H, H-8), 8.21 (s, 1H, H-2), 6.30 (d, J=2.7 Hz, 1H, H-4′), 4.11 (s, 2H, CH$_2$OH), 3.76 (s, 2H, H-2′a,b), 2.04−2.10 (m, 1H, H-5′), 1.13 (t, J=4.6 Hz, 1H, H-6′a), 1.00 (dd, J=7.7, 5.2 Hz, 1H, H-6′b); δ_C (62.5 MHz, MeOH-d_4) 157.4, 154.0, 150.5, 140.0, 120.2, 86.3, 72.2, 63.5, 33.2, 25.8, 11.9; δ_C (100 MHz, CD$_3$OD) 156.8, 152.7, 149.5, 138.8, 118.8, 85.0, 70.8, 62.2, 31.8, 24.4, 10.5; FAB-MS m/z 248 (MH$^+$, 100%), 136 (b+2H$^+$, 43), 113 (26). Elemental analysis for C$_{11}$H$_{13}$N$_5$O$_2$·1.15H$_2$O: calculated: C, 49.52; H, 5.35; N, 26.24. Found: C, 49.78; H, 5.31; N, 26.05.

4.7.8. [(2R,3S)-3-(tert-Butyldimethylsilyloxy)-5-methoxytetrahydrofuran-2-yl]methanol (11).
A stirred solution of compound **10**[11] (8.6 g, 34 mmol) in dry DMF (100 mL) was reacted with tert-butyldimethylsilyl chloride (8.8 g, 58 mmol) and imidazole (7.0 g, 102 mmol) at room temperature for 20 h. After the addition of EtOAc (200 mL), the organic phase was washed with water (2×100 mL), dried (MgSO$_4$), and reduced to dryness. The crude product was taken up in CH$_2$Cl$_2$ (80 mL) and treated with a 25% solution of NaOMe in methanol (10 mL). After stirring for 1 h at room temperature, the entire mixture was loaded on a silica gel column and then purified by flash chromatography (10→25% EtOAc in hexanes) to give **11** (7.85 g, 87.7%) as an oily, 1:1 mixture of isomers:

A and B; δ_H (400 MHz, CDCl$_3$) 5.02 (dd, J=5.6, 1.8 Hz, 0.5H, H-5$_A$), 4.92 (dd, J=5.9, 3.1 Hz, 0.5H, H-5$_B$), 4.43 (m, 0.5H, H-3$_A$), 4.13 (m, 0.5H, H-3$_B$), 3.95 (irregular q, J=6.7, 4.0 Hz, 0.5H, H-2$_A$), 3.81 (m, 1H, CHHOH$_A$, H-2$_B$), 3.68 (dd, J=11.9, 2.5 Hz, 0.5H, CHHOH$_A$), 3.56 (dd, J=12.5, 4.4 Hz, 0.5H, CHHOH$_B$), 3.53 (dd, J=12.1, 3.6 Hz, 0.5H, CHHOH$_B$), 3.30 (s, 1.5H, OCH$_{3/A}$), 3.29 (s, 1.5H, OCH$_{3/B}$), 2.36 (ddd, J=13.8, 8.6, 6.5 Hz, 0.5H, H-4′$_A$), 2.13 (ddd, J=13.5, 6.8, 1.7 Hz, 0.5H, H-4″$_A$), 2.01 (dt, J=13.5, 5.8 Hz, 0.5H, H-4′$_B$), 1.77 (ddd, J=13.6, 6.1, 3.0 Hz, 0.5H, H-4″$_B$), 0.82 (s, 4.5H, C(CH$_3$)$_{3/A}$), 0.81 (s, 4.5H, C(CH$_3$)$_{3/B}$), 0.01 (s, 3H, SiCH$_{3/A}$), 0.00 (s, 3H, SiCH$_{3/B}$); δ_C (100 MHz, CDCl$_3$, A/B isomers) 110.4/109.3, 92.6/88.2, 76.7/75.7, 68.1/66.3, 60.2/60.0, 47.7/46.9, 30.64/(overlapped), 22.85/22.83, 0.24/0.02; FAB-MS m/z 231 (MH$^+$−CH$_3$OH, 100%), 263 (MH$^+$, 2). Elemental analysis for C$_{12}$H$_{26}$O$_4$Si: calculated: C, 54.92; H, 9.99. Found: C, 54.70; H, 10.06.

4.7.9. (2S,3S)-Methyl 3-hydroxy-5-methoxytetrahydrofuran-2-carboxylate (12).
A solution of **11** (2.93 g, 11.61 mmol) in acetonitrile/water (1:1, 160 mL) was treated with bis(acetoxy)iodobenzene and

2,2,6,6-tetramethyl-1-piperidiyloxyl (TEMPO, 0.41 g, 2.62 mmol) and stirred at room temperature for 5 h. The solvents were removed under reduced pressure and the residue was co-evaporated twice with MeOH (10 mL). After adding 1.2 M HCl in methanol (70 mL), also at room temperature, the solution was stirred for 20 h. The solvent was removed under reduced pressure and the residue was purified by silica gel flash chromatography (33→50% EtOAc in hexanes) to give **12** (1.49 g, 73%) as an oily, 2:1 mixture of isomers; δ_H (400 MHz, CDCl$_3$, major isomer) 5.25 (dd, J=4.5, 0.6 Hz, 1H, H-5), 4.62 (d, J=1.6 Hz, 1H, H-2), 4.34 (overlapped s and d, J=4.5 Hz, 1H, OH, H-3), 3.74 (s, 3H, COCH_3), 3.40 (s, 3H, CHOCH_3), 2.00–2.15 (m, 2H, H-4a,b); δ_C (100 MHz, CDCl$_3$, A/B isomers) 172.2/171.0, 106.2/105.9, 85.1/83.5, 74.6/73.8, 55.3/55.1, 52.3/52.1, 41.1/40.0; ESI-FIA MS m/z 194 (M+NH$_4^+$, 100%), 145 (MH$^+$−CH$_3$OH). Elemental analysis for C$_7$H$_{12}$O$_5$·0.25H$_2$O: calculated: C, 46.53; H, 6.97. Found: C, 46.30; H, 7.06.

4.7.10. Methyl 5-methoxy-4,5-dihydrofuran-2-carboxylate (**13**).

A solution of **12** (1.06 g, 6.01 mmol) in anhydrous pyridine (30 mL) was stirred and cooled to −20 °C. Methanesulfonyl chloride (1.6 mL, 20.66 mmol) was added slowly, stirred for 2 h and stored in the freezer for 20 h. The solvent was removed under reduced pressure and the crude was immediately dissolved in anhydrous acetonitrile (30 mL), treated with 1,8-diazabicyclo[5.4.0]undec-7-ene (DBU, 5 mL, 33.2 mmol) and heated at 80 °C for 2 h.

After removing the solvents under reduced pressure, the crude product was purified twice by silica gel flash column chromatography (10→25% EtOAc in hexanes) to give **13** (0.713 g, 75%, single isomer) as an oil; δ_H (400 MHz, CDCl$_3$) 5.90 (dd, J=3.1, 2.7 Hz, 1H, H-3), 5.48 (dd, J=7.0, 2.3 Hz, 1H, H-5), 3.75 (s, 3H, COCH_3), 3.43 (s, 3H, CHOCH_3), 2.88 (ddd, J=18.7, 7.2, 2.7 Hz, 1H, H-4a), 2.52 (ddd, J=18.5, 3.1, 2.5 Hz, 1H, H-4b); δ_C (100 MHz, CDCl$_3$) 160.4, 146.2, 110.3, 106.6, 55.7, 51.9, 37.2. The elemental analysis for this compound was off (found: C, 49.83; H, 6.08; C$_7$H$_{10}$O$_4$·0.5H$_2$O requires C, 50.30; H, 6.63%) and the major peak in the mass spectrum corresponded to the aromatic furan. The appearance of the sample, however, was very pure by RP HPLC (single peak, MeOH/H$_2$O, 1:1).

4.7.11. rel-(1S,3S,5S)-Methyl 3-methoxy-2-oxabicyclo[3.1.0]hexane-1-carboxylate [(±)-**14**].

Compound **13** (1.35 g, 8.53 mmol) was treated with a solution of freshly prepared diazomethane in ether (200 mL) and the resulting solution was stirred at room temperature for 20 h (the diazomethane solution was prepared by the standard procedure starting from 16 g of Diazald®.) After removing the solvent under reduced pressure, the crude residue was dissolved in a 1:1 mixture of acetonitrile and benzene (60 mL). Following the addition of benzophenone (0.70 g) the flask was placed inside a photochemical reactor for 2 h. After removing the flask and allowing it to reach room temperature, the solvent was removed under reduced pressure and the residue was purified by silica gel flash column chromatography (5→25% EtOAc in hexanes) to give (±)-**14** (1.07 g, 73%) as a clear oil; δ_H (400 MHz, CDCl$_3$) 5.22 (d, J=6.3 Hz, 1H, H-3), 3.72 (s, 3H, COCH_3), 3.27 (s, 3H, OCH_3), 2.29 (ddd, J=13.5, 7.2, 1.1 Hz, 1H, H-4a), 2.01 (dt, J=12.1, 9.3 Hz, 1H, H-5), 1.90 (d, J=13.5 Hz, 1H, H-4b), 1.48 (ddd, J=9.3, 5.5, 1.1 Hz, 1H, H-6a), 1.43 (t, J=6.0 Hz, 1H, H-6b); δ_C (100 MHz, CDCl$_3$) 171.5, 108.4, 67.37, 55.1, 52.1, 35.2, 26.1, 22.8; APCI-FIA MS m/z 173 (MH$^+$, 90%). Elemental analysis for C$_8$H$_{12}$O$_4$: calculated: C, 55.81; H, 7.02. Found: C, 55.59; H, 7.12.

4.7.12. [rel-(1S,3S,5S)-3-Methoxy-2-oxabicyclo[3.1.0]hexan-1-yl]methyl acetate [(±)-**15**].

An iced-cold solution of (±)-**14** (0.57 g, 3.31 mmol) in anhydrous THF (50 mL) was stirred and treated with 1 M solution of lithium aluminum hydride (LAH, 5.40 mL). After 5 min, the cooling bath was removed and stirring was continued for 1 h. The mixture was diluted with EtOAc (100 mL) and carefully

washed with water (50 mL). The organic layer was dried (MgSO$_4$) and concentrated under reduced pressure. The crude product was immediately dissolved in anhydrous pyridine (50 mL) and treated with acetic anhydride (8 mL, 84.6 mmol) and stirred overnight. After the addition of EtOAc (100 mL) the organic layer was washed with water (2×50 mL), dried (MgSO$_4$), and reduced to dryness at under vacuum. The crude product was purified by silica gel flash column chromatography (5→25% EtOAc in hexanes) to give (±)-**15** (0.33 g, 53.6%) as a clear oil; δ_H (400 MHz, CDCl$_3$) 5.10 (d, J=5.9 Hz, 1H, H-3), 4.35 (d, J=12.7 Hz, 1H, CH*HOAc), 4.18 (dd, J=12.5, 0.6 Hz, 1H, C*HHOAc), 3.25 (s, 3H, COCH_3), 2.26 (ddd, J=13.5, 6.2, 1.1 Hz, 1H, H-4a), 2.04 (s, 3H, CHOCH_3), 1.87 (d, J=13.3 Hz, 1H, H-4b), 1.43 (dt, J=9.3, 5.2 Hz, 1H, H-5), 1.11 (t, J=5.4 Hz, 1H, H-6a), 0.70 (ddd, J=9.2, 6.1, 1.1 Hz, 1H, H-6b); δ_C (100 MHz, CDCl$_3$) 171.0, 107.7, 68.2, 66.6, 54.9, 36.2, 20.9, 18.9, 18.1; APCI-FIA MS m/z 187 (MH$^+$, 80%). Elemental analysis for C$_9$H$_{14}$O$_4$: calculated: C, 58.05; H, 7.58. Found: C, 58.20; H, 7.63.

4.7.13. [rel-(1S,5S)-3-(Acetyloxy)-2-oxabicyclo[3.1.0]hexan-1yl] methyl acetate [(±)-**16**].

Acetic anhydride (0.9 mL, 9.52 mmol) was added to a solution of (±)-**15** (0.166 g, 0.89 mmol) in acetic acid (6 mL) at 0 °C. Sulfuric acid (0.01 mL) was then added and the solution was stirred at room temperature for 2 h. Water (20 mL) was added and the aqueous phase was extracted with CH$_2$Cl$_2$ (2×70 mL). The organic phase was washed with saturated aqueous NaHCO$_3$ (50 mL), water (50 mL), and dried (MgSO$_4$). After removing the solvent under reduced pressure the crude product was purified by silica gel flash chromatography (10→33% EtOAc in hexanes) to give (±)-**16** (0.112 g, 59.3%) as an oily mixture (2:1) of isomers; δ_H (400 MHz, CDCl$_3$, 2:1 A/B isomers) 6.38 (d, J=6.3 Hz, H-3$_A$), 6.04 (d, J=4.9 Hz, H-3$_B$), 4.31 (AB q, J=12.7 Hz, CH$_2$OAc$_A$), 4.29 (AB q, J=12.7 Hz, CH$_2$OAc$_B$), 2.42 (m, H-4$_A$), 2.24 (br dd, J=6.8, 14.4 Hz, H-4$_B$), 2.12 (br ddd, J=5.2, 2.0, 14.4 Hz, H-4′$_B$), 2.04 (s, COC$H_{3/A}$), 2.03 (s, COC$H_{3/B}$), 2.02 (m, H-4′$_A$), 2.00 (s, COC$H_{3/A}$), 1.97 (s, COC$H_{3/B}$), 1.65 (m, H-5$_A$), 1.54 (m, H-5$_B$), 1.11 (br t, J 5.8 Hz, H-6$_A$), 0.99 (dd, J=6.0, 9.2 Hz, H-6$_B$), 0.81 (dd, J=6.8, 9.2 Hz, H-6′$_A$), 0.69 (br t, J 5.6 Hz, H-6′$_B$); δ_C (100 MHz, CDCl$_3$, major isomer) 170.05, 168.86, 99.06, 68.53, 64.92, 34.73, 23.24, 20.41, 17.74, 16.72; APCI-FIA MS m/z 232 (M+NH$_4^+$, 85%). Elemental analysis for C$_{10}$H$_{14}$O$_5$: calculated: C, 56.07; H, 6.59. Found: C, 56.05; H, 6.63.

4.7.14. [rel-(1S,3R,5S)-3-(6-Aminopurin-9-yl)-2-oxabicyclo[3.1.0]hexan-1-yl]methyl acetate [(±)-**17**].

A stirred suspension of adenine (86 mg, 0.64 mmol) and (±)-**16** (84.6 mg, 0.39 mmol) in dry acetonitrile (5 mL) at room temperature was treated cautiously with SnCl$_4$ (0.11 mL). After 30 min, pyridine (2 mL) was added and the mixture was further diluted with CHCl$_3$ (150 mL). The organic solution was washed with saturated aqueous NaHCO$_3$ (50 mL), water (50 mL), and dried (MgSO$_4$). The filtered solution was concentrated under reduced pressure and the residue was purified by silica gel flash column chromatography (10→33% EtOAc in hexanes) followed by (2→10% MeOH in CH$_2$Cl$_2$) to give 0.80 g (70.2%) of (±)-**17** plus 20% of the α-isomer as a foam; δ_H (400 MHz, CDCl$_3$, major isomer) 8.28 (s, 1H, H-8), 8.02 (s, 1H, H-2), 6.12 (dd, J=7.2, 4.8 Hz, 1H, H-3′), 4.25 (AB q, J=12.7 Hz, 2H, CH$_2$OAc), 2.73 (m, 1H, H-4′a), 2.64 (m, 1H, H-4′b), 1.99 (s, 3H, COCH_3), 1.84 (m, 1H, H-5′), 0.62 (m, 2H, H6′a, H6′b); δ_C (100 MHz, CDCl$_3$, major isomer), 169.88, 154.60, 152.15, 151.96, 137.56, 112.56, 85.74, 68.02, 64.02, 35.62, 19.82, 18.58, 18.11; FAB-MS m/z 290 (MH$^+$, 100%), 136 (b+2H$^+$, 70). This inseparable mixture of isomers was used as such in the next step.

4.7.15. N-{9-[rel-(1S,3R,5S)-1-(Hydroxymethyl)-2-oxabicyclo[3.1.0]hexan-3-yl]purin-6-yl}benzamide [(±)-**18**].

A stirred suspension of the mixture of isomers [(±)-**17** α-isomer, 213 mg, 0.74 mmol] in saturated methanolic ammonia (70 mL) was stirred in a sealed vessel at room temperature for 48 h. The solvent was removed

under reduced pressure and the crude product was purified, first by silica gel column chromatography (2→20% MeOH in CH$_2$Cl$_2$), followed by C-18 reversed phase column chromatography (water→5% MeOH in water→50% MeOH in water) to give 163 mg (86.2%) of a mixture of isomers. A stirred solution of the mixture of isomers (148 mg, 0.59 mmol) in dry pyridine (25 mL) was treated with tri-methylsilyl chloride (TMSCl, 1.3 mL, 10.25 mmol). After 30 min stirring at room temperature, benzoyl chloride (1 mL, 8.6 mmol) was added and stirring continued for 2 h. Following cooling the solution over ice, water (3 mL), and concentrated NH$_4$OH (10 mL) were added. The ice bath was removed, stirring continued for 40 min, and the solution was concentrated under reduced pressure. The residue was dissolved in water (40 mL) and washed with ethyl ether (2×20 mL) and then lyophilized. The crude product was pu-rified by silica gel flash column chromatography (50% EtOAc in hexanes→100% EtOAc→3% MeOH in CH$_2$Cl$_2$→10% MeOH in CH$_2$Cl$_2$) to give (±)-**18** (82.4 mg, 39%). The solid was recrystallized (MeOH/CH$_2$Cl$_2$) and dried under vacuum to give 68.8 mg of pure product; mp 184–185 °C; δ_H (400 MHz, CDCl$_3$) δ 9.00 (br s, 1H, CON*H*), 8.72 and 8.10 (br singlets, 2H, H-2, and H-8), 7.96 (d, *J*=7.6 Hz, 2H, Ph), 7.55 (t, *J*=7.2 Hz, 1H, Ph), 7.46 (irregular t, *J*=7.6 Hz, 2H, Ph), 6.06 (dd, *J*=7.2, 5.6 Hz, 1H, H-3), 4.32 (d, *J*=13.6 Hz, 1H, C*H*HOH), 3.44 (d, *J*=13.6 Hz, 1H, CH*H*OH), 2.77 (dd, *J*=13.6, 7.6 Hz, 1H, H-4a), 2.67 (dd, *J*=13.6, 6.0 Hz, 1H, H-4b), 1.85 (m, 1H, H-5), 0.89 (m, 2H, H-6a,b); δ_C (100 MHz, CDCl$_3$), 164.51, 152.60, 141.41, 133.48, 132.84, 128.87, 127.85, 113.46, 87.76, 72.57, 64.24, 36.88, 18.46, 17.94; FAB-MS *m/z* 352 (MH$^+$, 65%), 240 (b+2H$^+$, 100). Elemental analysis for C$_{18}$H$_{17}$N$_5$O$_3$: calculated: C, 61.53; H, 4.88; N 19.95. Found: C, 61.26; H, 4.91; N, 19.80.

The small amount obtained of the ∠-isomer was treated im-mediately with saturated methanolic ammonia as for the major isomer in the final step (see below).

4.7.16. [rel-(1S,3R,5S)-3-(6-Aminopurin-9-yl)-2-oxabicyclo[3.1.0] hexan-1-yl]methanol [(±)-2]. A stirred suspension of (±)-**18** (38 mg, 0.10 mmol) in saturated methanolic ammonia (15 mL) was stirred in a sealed vessel at room temperature for 48 h. The solvent was removed under reduced pressure and the crude product was purified by silica gel flash column chromatography to give 25.3 mg (94.7%) of the β-isomer, which was recrystallized (MeOH/CH$_2$Cl$_2$) as a white solid, mp 197–198 °C; UV λ_{max} (EtOH)/261 nm; δ_H (400 MHz, D$_2$O) 8.38 (s, 1H, H-8), 8.24 (s, 1H, H-2), 6.23 (dd, *J*=7.3, 4.9 Hz, 1H, H-3), 3.97 (d, *J*=13.1 Hz, 1H, C*H*HOH), 3.70 (d, *J*=13.1 Hz, 1H, CH*H*OH), 2.84 (ddd, *J*=14.3, 6.5, 4.9 Hz, 1H, H-4a), 2.53 (ddd, *J*=14.3, 7.5, 1.0 Hz, 1H, H-4b), 1.98 (ddd, *J*=14.7, 6.6, 1.4 Hz, 1H, H-5), 1.00 (d, *J*=7.2 Hz, 2H, H-6a,b); δ_C (100 MHz, CDCl$_3$) 155.3, 152.4, 148.2, 140.0, 118.5, 86.8, 71.6, 63.15, 35.1, 18.4, 18.2; APCI-FIA MS *m/z* 248 (M$^+$, 100%); 136 (b+2H$^+$, 10). Elemental analysis for C$_{11}$H$_{13}$N$_5$O$_2$·0.1H$_2$O: calculated: C, 53.05; H, 5.34; N, 28.12. Found: C, 52.95; H, 5.28; N, 27.78.

α-isomer δ_H (400 MHz, D$_2$O) 8.35 (s, 1H, H-8), 8.25 (s, 1H, H-2), 6.64 (dd, *J*=7.9, 5.4 Hz, 1H, H-3), 4.07 (d, *J*=13.1 Hz, 1H, C*H*HOH), 3.71 (d, *J*=13.1 Hz, 1H, CH*H*OH), 2.99 (ddd, *J*=14.5, 7.3, 0.5 Hz, 1H, H-4a), 2.69 (dd, *J*=14.3, 5.3 Hz, 1H, H-4b), 1.90 (ddd, *J*=15.3, 7.0, 1.0 Hz, 1H, H-5), 1.13 (m, 2H, H-6a,b).

Acknowledgements

Supplementary data

Supplementary data containing the plot of pH versus ^{1}H chemical shifts for compounds (±)-**1** and (±)-**2** (Fig. 1S); HPLC conditions for the depurination kinetics; and complete crystallographic data on compound (±)-**1**, including crystal data and structure refinement, atomic coordinates, bond lengths and angles, anisotropic displace-ment parameters, hydrogen coordinates and isotropic displacement parameters, torsion angles, and hydrogen bonds (Tables S1–7). Supplementary data associated with this article can be found in the online version at doi:10.1016/j.tet.2010.06.044. These data include MOL files and InChIKeys of the most important compounds described in this article.

References and notes

1. Thibaudeau, C.; Acharya, P.; Chattopadhyaya, J. *Stereoelectronic Effects in Nu-cleosides and Nucleotides and their Structural Implications*; Uppsala University: Uppsala-Sweden, 2005, Chapter 1, pp 8–20.
2. For a detailed discussion about the anomeric effect, see Juaristi, E.; Cuevas, G. *The Anomeric Effect*; CRC: Boca Raton-Ann Arbor-London-Tokyo, 1995.
3. Jagannadh, B.; Reddy, D. V.; Kunwar, A. C. *Biochem. Biophys. Res. Commun.* **1991**, *179*, 386–391.
4. Plavec, J.; Koole, L. H.; Chattopadhyaya, J. *J. Biochem. Biophys. Methods* **1992**, *25*, 253–272.
5. Marquez, V. E. In *The properties of Locked Methanocarba Nucleosides in Bio-chemistry, Biotechnology and Medicine in Modified Nucleosides in Biochemistry, Biotechnology and Medicine*; Herdewijn, P., Ed.; Wiley-VCH: Weinheim, 2008; Chapter 12, pp 307–341.
6. Part of this work was presented as a poster at the XVIII International Round Table for Nucleosides, Nucleotides and Nucleic Acids, Kyoto, Japan, September 8–11, 2008: Marquez, V. E.; Sun, G.; Siddiqui, M. A.; Lee, Y.-C.; Barchi, J. J., Jr.; Filippov, I.; Landsman, N. A.; Kelley, J. A. *Nucleic Acids Symposium Series No. 52* **2008**, *543*–544.
7. Jeong, L. S.; Lee, Y. A.; Moon, H. R.; Chun, M. W. *Nucleosides Nucleotides* **1998**, *17*, 1473–1478.
8. Takahashi, H.; Yoshioka, M.; Ohno, M.; Kobayashi, S. *Tetrahedron Lett.* **1992**, *33*, 2575–2578.
9. Omura, K.; Swern, D. *Tetrahedron* **1978**, *34*, 1651–1660.
10. Vorbrügge, H.; Ruh-Pohlenz, C. *Handbook of Nucleoside Synthesis*; John Wiley: New York, NY, 2001.
11. Fedorov, I. I.; Kaz'mina, E. M.; Novicov, N. A.; Gurskaya, G. V.; Bochkarev, A. V.; Yas'ko, M. V.; Viktorova, L. S.; Kukhanova, M. K.; Balzarini, J. *J. Med. Chem.* **1992**, *35*, 4567–4575.
12. Ichikawa, Y.; Kubota, H.; Fujita, K.; Okauchi, T.; Narasaka, K. *Bull. Soc. Chem. Jpn.* **1989**, *62*, 845–852.
13. Vatèle, J.-M. *Tetrahedron Lett.* **2006**, *47*, 715–718.
14. Ti, G. S.; Gaffney, B. L.; Jones, R. A. *J. Am. Chem. Soc.* **1982**, *104*, 1316–1329.
15. Siddiqui, M. A.; Ford, H., Jr.; George, C.; Marquez, V. E. *Nucleosides Nucleotides* **1996**, *15*, 235–250.
16. NBO 5.0; Glendening, E. D.; Badenhoop, J. K.; Reed, A. E.; Carpenter, J. E.; Bohmann, J. A.; Morales, C. M.; Weinhold, F. Theoretical Chemistry Institute, University of Wisconsin, Madison; 2001; http://www.chem.wisc.edu/~nbo5/.
17. The value of *P* indentifies the conformation of the sugar (or pseudosugar) ring in the pseudorotational wheel (0°→360°). The North conformations encom-pass a range between 342° and 18° ($_2$E→^{3}T$_2$→^{3}E), where E and T correspond to envelope (E) and twisted (T) conformations of the five-member ring, and the super- or subscripts denote the atoms that project above or below the plane of the ring. The antipodal South conformations oscillate between 162° and 198° (^{2}E→$_3$T^2→$_3$E). The pure North (^{3}T$_2$) or South ($_3$T^2) conformations correspond to 0° and 180° in the pseudorotational cycle. Because of the rigid boat con-formation, the bicyclo[3.1.0]hexane scaffold locks the positions of the embed-ded ring at $_2$E (342°) and $_3$E (198°), respectively.
18. Plavec, J.; Tong, W.; Chattopadhyaya, J. *J. Am. Chem. Soc.* **1993**, *115*, 9734–9746.
19. Thibaudeau, C.; Plavec, J.; Chattopadhyaya, J. *J. Org. Chem.* **1996**, *61*, 266–286.
20. Stonehouse, J.; Adell, P.; Keeler, J.; Shaka, A. J. *J. Am. Chem. Soc.* **1994**, *116*, 6037–6038.
21. Gaussian 98 Frisch, M. J.; Trucks, G. W.; Schlegel, H. B.; Scuseria, G. E.; Robb, M. A; Stratmann, R. E.; Burant, J. C.; Dapprich, S.; Millam, J. M.; Daniels, A. D.; Kudin, K. N.; Strain, M. C.; Farkas, O.; Tomasi, J.; Barone, V.; Cossi, M.; Cammi, R.; Mennucci, B.; Pomelli, C.; Adamo, C.; Clifford, S.; Ochterski, J.; Petersson, G. A.; Ayala, P. Y.; Cui, Q.; Morokuma, K.; Salvador, P.; Dannenberg, J. J.; Malick, D. K.; Rabuck, A. D.; Raghavachari, K.; Foresman, J. B.; Cioslowski, J.; Ortiz, J. V.; Baboul, A. G.; Stefanov, B. B.; Liu, G.; Liashenko, A.; Piskorz, P.; Komaromi, I.; Gomperts, R.; Martin, R. L.; Fox, D. J.; Keith, T.; Al-Laham, M. A.; Peng, C. Y.; Nanayakkara, A.; Challacombe, M.; Gill, P. M. W.; Johnson, B.; Chen, W.; Wong, M. W.; Andres, J. L.; Gonzalez, C.; Head-Gordon, M.; Replogle, E. S.; Pople, J. A. *Gaussian 98*; Gaussian: Pittsburgh, PA, 1998.
22. Frisch, M. J.; Trucks, G. W.; Schlegel, H. B.; Scuseria, G. E.; Robb, M. A.; Cheeseman, J. R.; Montgomery, J. A., Jr.; Vreven, T.; Kudin, K. N.; Burant, J. C.; Millan, J. M.; Iyengar, S. S.; Tomasi, J.; Barone, V.; Mennucci, B.; Cossi, M.;

Scalmani, G.; Rega, N.; Peterson, G. A.; Nakatsuji, H.; Hada, M.; Ehara, M.; Toyota, K.; Fukuda, R.; Hasegawa, J.; Ishida, M.; Nakajima, T.; Honda, Y.; Kitao, O.; Nakai, H.; Klene, M.; Li, X.; Knox, J. E.; Hratchian, H. P.; Cross, J. B.; Bakken, V.; Adamo, C.; Jaramillo, J.; Gomperts, R.; Stratmann, R. E.; Yazyev, O.; Austin, A. J.; Cammi, R.; Pomelli, C.; Ochterski, J. W.; Ayala, P. Y.; Morokuma, K.; Voth, G. A.; Salvador, P.; Dannenberg, J. J.; Zakrzewski, V. G.; Dapprich, S.; Daniels, A. D.; Strain, M. C.; Farkas, O.; Malick, D. K.; Rabuck, A. D.; Raghavachari, K.; Foresman, J. B.; Oriz, J. V.; Cui, Q.; Baboul, A. G.; Clifford, S.; Cioslowski, J.; Stefanov, B. B.; Liu, G.; Liashenko, A.; Piskorz, P.; Komaroni, I.; Martin, R. L.; Fox, D. J.; Keith, T.; Al-Laham, M. A.; Peng, C. Y.; Nanayakkara, A.; Challacombe, M.; Gill, P. M. W.; Johnson, B.; Chen, W.; Wong, M. W.; Gonzalez, C.; Pople, J. A. *Gaussian 03, Revision E.01*; Gaussian: Wallingford, CT, 2004.